Int. J. Electrochem. Sci., 7 **(2012)** 1266 - 1287

International Journal of
ELECTROCHEMICAL
SCIENCE
www.electrochemsci.org

Potentiodynamic and Quantum Studies of Some Amino Acids as Corrosion Inhibitors for Copper

H.H. Abdel Rahman[1], *A.H.E. Moustafa*[1,*], *M.K. Awad*[2]

[1] Chemistry Department, Faculty of Science, Alexandria University, Alexandria, Egypt
[2] Chemistry Department, Theoretical Applied Chemistry Unit (TACU), Faculty of Science, Tanta University, Tanta, Egypt
[*]E-mail: amirahossameldin@yahoo.com

Received: 21 November 2011 / *Accepted:* 29 December 2011 / *Published:* 1 February 2012

A comparative study of different types of amino acids: proline, cysteine, phenyl alanine, alanine, hisitidine and glycine as inhibitors for copper corrosion in 8*M* phosphoric acid at different temperatures was carried out. Potentiodynamic polarization and rotation techniques were applied to study the metal corrosion behaviour in the absence and presence of different concentrations of theses inhibitors. The results reveal that amino acids have strongest inhibitive effects that provide good protection to copper surface against corrosion in acid solutions. Adsorption of amino acids on copper surface, in 8*M* phosphoric acid solution, follows Temkin adsorption isotherm model. The $\Delta G_{ads.}$ values were calculated and indicated physical adsorption. Quantum chemical parameters were calculated using semiempirical PM6 method to find a good correlation with the inhibition efficiency. A good correlation was found between the theoretical calculations and experimental observations.

Keywords: Copper corrosion; Amino acids; Adsorption isotherm; polarization; Quantum chemical calculations.

1. INTRODUCTION

Chemical, physical and mechanical properties of copper make it the world third most widely used metal after iron and aluminium. It is used in very essential fields such as electrical applications, building constructions, industrial machinery, equipment, transportation, and consumer products [1].

The corrosion of metals is a common phenomenon in industry, and it has received a considerable amount of attention. The use of inhibitors is one of the most practical methods for protection against corrosion. Usually, organic compounds are widely used in industry for preventing corrosion in acidic environments [2-8].

To improve the protective efficiency of copper corrosion in corrosive environment, great efforts have been put into the investigation and lots of technologies have been used [9-11]. The inhibitive power of the organic inhibitors has been interpreted in term of many different characteristics such as molecular size, molecular weight, molecular structure, nature of heteroatom present in the molecule, etc. [2]. Nitrogen containing compounds have been found to serve as good inhibitors of corrosion [12] and their inhibiting action has been explained in term of the number of mobile electron pairs [13], the π orbital character of free electron, and the electron density around the nitrogen atom [2]. Among numerous inhibitors that have been tested and are applied industrially as corrosion inhibitors, those that are non-toxic or low-toxic are now far more strategic than in the recent past [14]. Amino acids are known to be very effective non toxic inhibitors for metal and alloys in different corrosion media. The process is diffusion controlled, depending on the concentration gradient forming a selective electrochemical dissolution of copper. The limiting current value that determines the corrosion efficiency depends on the rate of mass transfer of Cu^{2+} ions from the diffusion layer to the bulk of the solution. The rate of mass transfer depends on the relative ionic movement, geometry of anode, temperature, the type and the physical properties of the electrolyte [1, 15]

This present work is aimed to study the inhibition efficiency of inhibitors and correlate their efficiency with the quantum chemical parameters of the investigated compounds. Experimental means are useful to explain the inhibition mechanism but they are often expensive and time-consuming. Ongoing hardware and software advances have opened the door for powerful use of theoretical chemistry in corrosion inhibition research. Several quantum chemical methods and molecular modeling techniques have been performed to correlate the inhibition efficiency of the inhibitors with their molecular properties [16-22].

2. EXPERIMENTAL

2.1. Chemicals

Analar grade H_3PO_4 (98% w/w), supplied by BDH Chemicals Ltd., were used for the preparation of the electrolyte. Amino acids used were: (i) proline I, (ii) cysteine II, (iii) phenyl alanine III, (iv) alanine IV, (v) hisitidine V, (vi) glycine VI. The choice of these compounds was based on molecular structure considerations; it's an organic compound with an adsorption center. The inhibitor molecules may lie on the copper surface with one adsorption center if the concentration of inhibitor is low enough.

2.2. Solution Composition

Blank solution consists of 8*M* H_3PO_4 and different concentrations of amino acids (I-VI). The concentrations of amino acids cover range from $1x10^{-6}$ to $1x\ 10^{-3}$ M.

2.3. Apparatus and Procedure

The cell consists of a rectangular plastic container having the dimensions (5.1x 5x10 cm) with electrodes fitting the whole cross section area. The electrodes were rectangular copper sheets of 10 cm height and 5 cm width, were located 5.1 cm apart. A porous Poly Vinyl Chloride (PCV) diaphragm was used to prevent the effect due to H_2 bubbles. The electrical circuit consists of 6 V D.C. power supply connected in parallel with the cell to measure the voltage and multi-range digital ammeter connected in series with the cell to measure the current. Reference electrode consists of a copper wire immersed in a cup of luggin tube filled with the phosphoric acid concentration similar to that in the cell, the tip of the luggin tube was placed 0.5 – 1mm from the anode. The potential difference between the anode and the reference electrode was measured by potentiometer. Phosphoric acid concentration was prepared from the Analar grade ortho- phosphoric acid and distilled water .The anode height was 1cm and before each run, the back part of the anode was insulated with epoxy resin and the active surface of the anode was polished with fin emery paper, degreased with trichloroethylene, washed with alcohol and finally rinsed in distilled water. Electrode treatment was similar to that used by Wilke [23]. The rate of copper corrosion under different conditions is determined by measuring the limiting current at 25 ^{o}C.

2.4. Density and Viscosity Measurements

The density was determined by using DA-300 Kyoto Electronics at 25, 30, 35 and 40 ±1 ^{o}C. An oscillation period of the measuring cell which is generated when it is given the natural oscillation, will vary depend on the density of the sample in the cell. The viscosity is measured using Koehler viscosity bathing (Model K23400 Kinematic Baths) at 25, 30, 35 and 40 ±1 ^{o}C.

2.5. Computational details

Complete geometrical optimizations of the investigated molecules were performed using semiempirical PM6 method implemented in MOPAC 2009. The calculated parameters are, the highest occupied molecular orbital (HOMO), the lowest unoccupied molecular orbital (LUMO), the separation energy (ΔE), the dipole moment (μ), the softness (σ), hardness (η), the total negative charge (TNC), and the total energy (E_t). Frontier molecular orbitals (HOMO and LUMO) could be used to predict the adsorption centers of the inhibitor molecule. According to Koopman's theorem [24], the E_{HOMO} and E_{LUMO} of the inhibitor molecule are related to the ionization potential, I, and the electron affinity A, respectively, by the following relations:

$$I = -E_{HOMO} \quad (1)$$

$$A = -E_{LUMO} \quad (2)$$

The calculated quantum chemical parameters, hardness, η and softness, σ were calculated [25]:

$$\eta = \frac{(E_{LUMO} - E_{HOMO})}{2} \quad (3)$$

The inverse of the global hardness is designated as the softness, σ as follows:

$$\sigma = {}^{1}/_{\eta} \quad (4)$$

3. RESULTS AND DISCUSSION

3.1. Levelling process

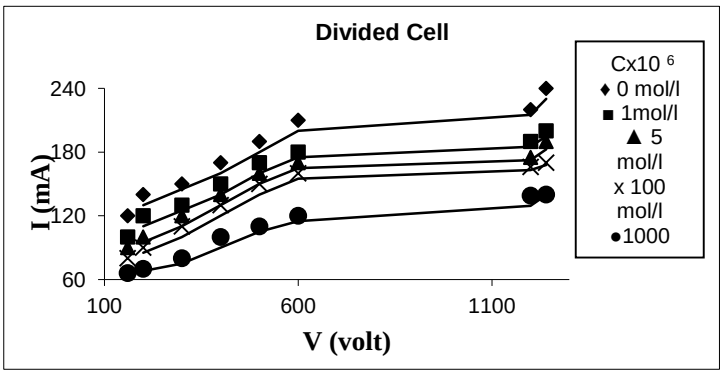

Figure 1. Limiting currents I (mA**)** with diaphragm in presence of different concentrations of compound (I) at 25 ^{o}C.

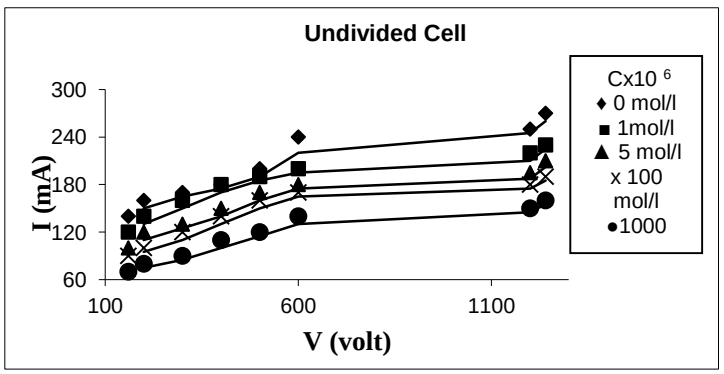

Figure 2. Limiting currents I (mA**)** without diaphragm in presence of different concentrations of compound (I) at 25^{o}C.

Levelling is the principle process in corrosion [26]. Mayer [27] explained the necessity to separate between anode and cathode by non conductive slit to prevent the gas bubbles transfer to the anode surface and enhance the homogenous distribution of electric current [1]. The study of levelling is based on the classical current voltage curves of electropolishing as shown in (Fig. 1&2) a typical polarogram is obtained in this study for amino acids in case of divided and undivided cell. The curve is divided into three parts: in the first part the current density (c.d.) is proportional to the voltage and etching takes place. At the second part of the curve, the metal undergoes corrosion and in the last part, some localized pitting occurs [28].

3.2. Effect of electrode height on limiting current

Fig. 3 shows that, the limiting current density decreases with the increases in height. In corrosion and generally for anodic dissolution of metal , the direction of flow of thermodynamic boundary layer and the diffusion layer increase in the downward direction , i.e. the resistance to mass transfer increase in the downward direction. Accordingly, the local limiting current density increasing in the up- ward direction of the anode.

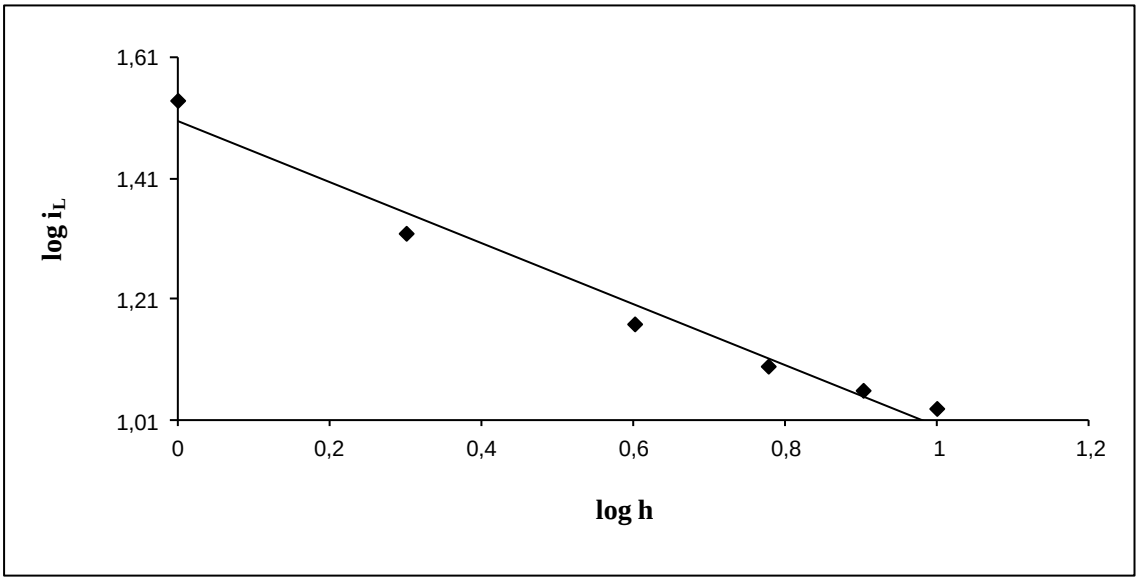

Figure 3. Effect of electrode height on the limiting current using compound (IV) at 25 ^{o}C**.**

This explains why corrosion is attained at the upper parts of the electrode before the lower parts at the limiting current region. This was confirmed by visual observation during corrosion process. The average limiting current density decreases with increase in the height according to the following equation [29]:

$$i_L = \frac{C}{(H)^a} \qquad (5)$$

where C is constant, H is the height of electrode, a is constant depends on the type of solution , [a= 0.502 for undivided cell].

3.3. Effect of amino acids concentration on the limiting current

The observed limiting current, which represent the rate of copper metal corrosion in orthophosphoric acid at 25 ^{o}C, are found that, the limiting current decrease with increasing the concentration of amino acids as shown in Table 1.

Table 1. The calculated limiting current (mA) for the corrosion of copper in the presence of amino acids (I-VI) at different temperatures and different concentration.

A-A-	Cx10^6 mol/l	I_L (mA)				Organic Compounds	Cx10^6 mol/l	I_L (mA)			
		298 K	303 K	308 K	313 K			298 K	303 K	308 K	313 K
Compound(I) (Proline)	0	230	240	255	270	**Compound(IV) (Alanine)**	0	230	240	255	270
	1	190	210	225	245		1	195	205	213	223
	5	175	190	210	225		5	180	187	195	202
	10	172	180	195	210		10	177	183	188	198
	50	170	172	180	195		50	175	183	190	195
	100	166	170	176	183		100	171	176	183	191
	500	147	160	170	178		500	152	157	162	169
	1000	139	145	160	170		1000	147	133	138	143
		298 K	303 K	308 K	313 K			298 K	303 K	308 K	313 K
Compound(II) (Cysteine)	0	230	240	255	270	**Compound(V) (Histidine)**	0	230	240	255	270
	1	155	163	168	175		1	140	145	150	160
	5	147	155	165	170		5	135	140	145	150
	10	145	147	155	160		10	130	135	140	145
	50	133	142	150	158		50	125	130	135	140
	100	126	133	140	150		100	120	125	130	136
	500	120	126	132	140		500	110	115	122	130
	1000	110	120	128	135		1000	105	110	117	122
		298 K	303 K	308 K	313 K			298 K	303 K	308 K	313 K
Compound(III) (Phenyl alanine)	0	230	240	255	270	**Compound(VI) (Glycine)**	0	230	240	255	270
	1	170	178	190	200		1	200	210	218	228
	5	160	170	180	196		5	185	192	200	207
	10	150	160	170	180		10	182	188	195	203
	50	140	150	160	170		50	180	188	193	198
	100	130	140	150	160		100	176	181	188	196
	500	125	132	140	150		500	157	162	167	175
	1000	120	125	130	140		1000	145	138	142	147

We can recommend on the basis of result, it may use in this range of concentration to inhibit the corrosion of copper metal in 8*M* H_3PO_4 acid in all type of amino acids to be used in this work [30].

The mass transfer coefficient of the corrosion process which was used in data correlation was calculated from the limiting current using the equation:

$$k = \frac{I}{ZFAC_s} \qquad (6)$$

The above equation is based on the finding of previous studies [31]. If the limiting current in absence (I), and presence of amino acids (I_l), the percentage of inhibition can be calculated from the following equation:

$$\%IE = \frac{I - I_l}{I} \times 100 \qquad (7)$$

Fig. 4 and Table 2 show that, the inhibition percent that caused by amino acids ranges from 13.04 % to 54.34 % depending on its type and concentration.

The limiting current decreases with increasing the concentration of amino acids this agree with the finding of other authors who worked within the same range of concentration using other anode geometries [32]. The decreasing in the limiting current with increasing the concentration of amino acids is attributed to the viscosity of organic additives water-H_3PO_4 mixture is higher than water-H_3PO_4 mixture, this led to: decrease in diffusivity of Cu^{2+} and the solubility of copper phosphate in organic additives mixture is lower than water phosphoric acid mixture, so the saturation of solution is attained quickly and limiting current is small [33, 34].

Table 2- % Inhibition efficiency of copper corrosion using 8*M* H_3PO_4 in presence of different concentrations of amino acids at 25 ^oC.

	IE%					
Cx10^6 mol/l	**I**	**II**	**III**	**IV**	**V**	**VI**
Blank	0.00	0.00	0.00	0.00	0.00	0.00
1	17.39	32.60	26.08	15.22	39.13	13.04
5	23.90	36.10	30.43	21.74	41.30	19.56
10	25.22	37.10	34.78	23.04	43.47	20.86
50	26.08	42.17	39.13	23.91	45.11	21.74
100	27.82	45.10	43.47	25.65	47.82	23.48
500	36.08	47.82	45.10	33.91	52.17	31.74
1000	39.60	52.17	47.82	36.00	54.34	32.90

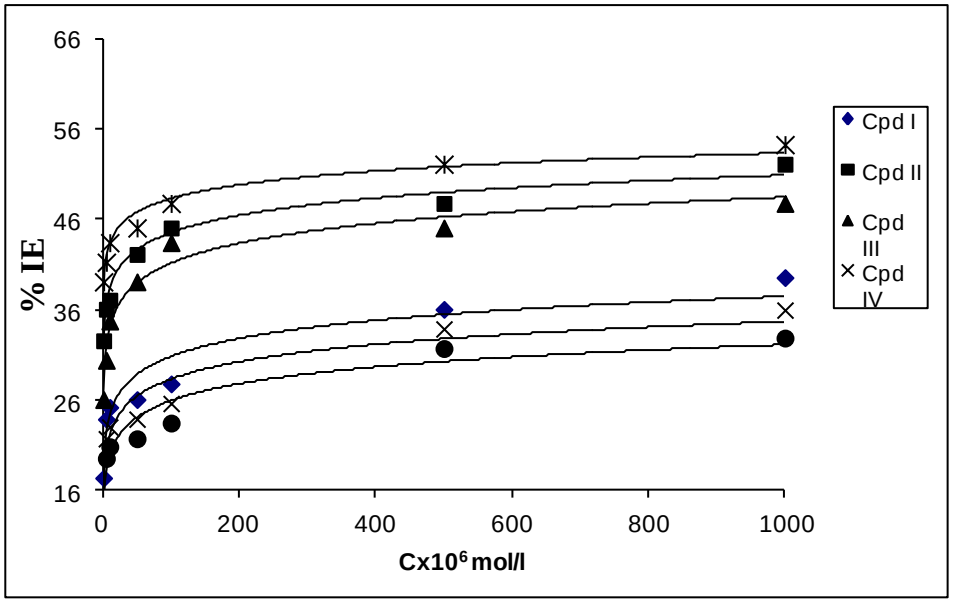

Figure 4. % Inhibition efficiency of copper corrosion using 8*M* H_3PO_4 in presence of different concentrations of amino acids at 25 ^oC.

3.4. Adsorption Isotherm

The amino acids compounds inhibit the corrosion of the copper by adsorbing onto the metal surface in acid solution. A useful method that assists in the understanding of the mechanism of organo-electrochemical reactions in the adsorption processes is the adsorption isotherm. The values of surface coverage (θ) corresponding to different concentrations of the inhibitor have been used to determine the adsorption isotherm. The Potentiodynamic polarization data were used to evaluate the surface coverage values as follows:

$$\theta = \frac{I_b - I_{org.}}{I_b} \qquad (8)$$

where I_b and $I_{org.}$ are the limiting current without and with amino acids, respectively [35]. The adsorption Langmiur has been tested for the description of the adsorption behaviour of the inhibitor. The linear correlation coefficients are good and all the slopes are not close to 1 meaning that the adsorption of inhibitor does not accord with the Langmiur adsorption isotherm [29]. In order to determine the mechanism of corrosion inhibition, the experimental data were applied to Temkin adsorption isotherm and it has the following general form:

$$Exp\ (-2a\theta) = KC \qquad (9)$$

where "a" is the lateral interaction parameter describing the molecular interaction in the adsorption layer and heterogeneity of the metal surface. From Fig. 5, for praline, cysteine, phenyl alanine, and histedine (as example), straight lines were obtained with slope1/- 2a and intercepts lnK/-2a, when θ was plotted against log C for the amino acids. The values of "a" -17.24, -17.98, -15.57, and -22.62 for amino acids respectively, are negative in all cases indicating that repulsion exists in the adsorption layer [2, 35].

The kinetic -thermodynamic model is given by:

$$\log \frac{\theta}{1-\theta} = \log K' + y \log C \qquad (10)$$

where y is the number of inhibitor molecules occupying one active site. The binding constant K is given by:

$$K = K'^{(1/y)} \qquad (11)$$

where 1/y is the number of the surface active sites occupied by one molecule of the inhibitor. Fig. 6 for praline, cysteine, phenyl alanine, and hisitidine (as example), linear relation between log θ / (1- θ) and log C at 25 ^{o}C, and the calculated values of 1/y and K are given in Table 3. The values of 1/y depend on the type of amino acids. The data of this Table reveals that, the values of 1/y for all amino acids higher than one i.e: the given inhibitors molecules are attached to more than one active site and at constant temperature [2, 36].

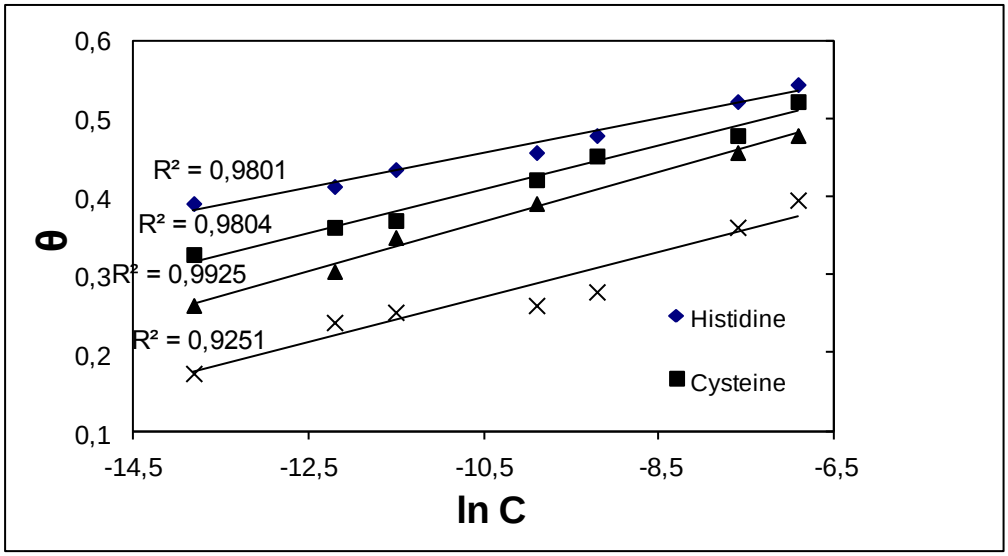

Figure 5. Curve fitting of corrosion data for Cu-Cu in 8*M* H_3PO_4 in the presence of different amino acids to Temkin isotherm at 25 ^{o}C.

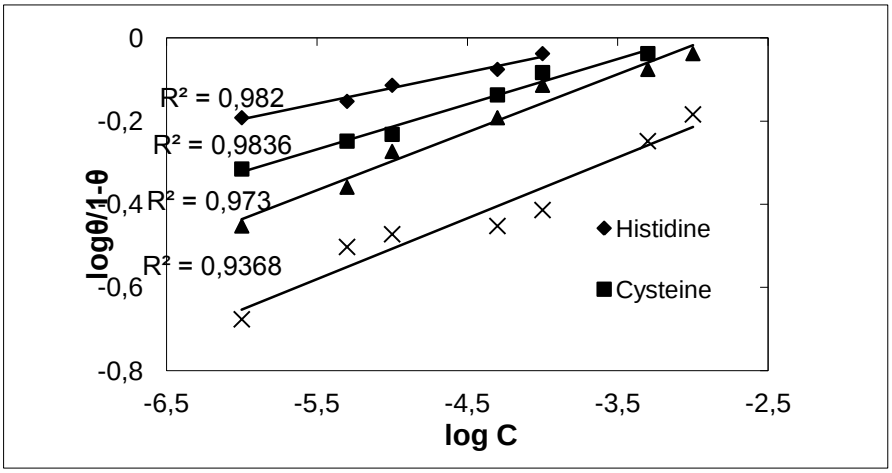

Figure 6. Curve fitting of corrosion data for Cu-Cu in 8*M* H_3PO_4 in the presence of different amino acids to the kinetic model at 25 ^oC.

The values of the free energy change for the adsorption process ($\Delta G_{ads.}$) for the different inhibitors at 25 ^oC were calculated from the following equation [2]:

$$\Delta G_{ads.} = -R\ T \ln (55.5\ K) \qquad (12)$$

The values of $\Delta G_{ads.}$ are collected in Table 3. It is clear from Table 3, that the adsorption free energies have negative values less than - 40 kJ mol^{-1}, meaning that the adsorption of the inhibitors molecules onto the copper surface in phosphoric acid is a spontaneous process and there is the electrostatic interaction between the charged inhibitor molecules and the charged metal surface (physical adsorption) [2, 14, 37]. The results show that histidine, cysteine and phenyl alanine which give maximum efficiency and show more negative free energy of adsorption than proline, alanine and glycine indicating that it is strongly adsorbed on the metal surface [38]

Table 3. Linear fitting parameters of amino acids at 25 ^oC.

Kinetic model			
A-A-	**1/y**	**K (L mol^{-1})**	**-ΔG (kJ mol^{-1})**
Histidine (V)	13.23	2.56E+03	29.39
Cysteine (II)	9.19	1.08E+03	26.98
Phenyl alanine (III)	7.15	7.55E+02	26.37
Proline (I)	6.83	34.32	18.71
Alanine (IV)	6.67	17.44	17.03
Glycine (VI)	6.42	9.72	15.58

3.5. Effect of Temperature

Table 4. Values of Thermodynamic parameters for different concentrations of amino acids.

A-A-	Cx10^6 mol/l	Ea (kJ mol^{-1})	ΔH* (kJ mol^{-1})	ΔS* (Jmol^{-1}K^{-1})	ΔG* (kJ mol^{-1})
Blank	0	8.41	5.93	-179.86	59.55
	1	12.92	10.44	-166.22	60.00
	5	13.27	10.79	-165.77	60.22
	10	10.52	8.05	-175.00	60.28
I	50	7.06	4.58	-186.98	60.33
	100	5.07	2.59	-193.74	60.36
	500	9.87	7.39	-178.52	60.63
	1000	15.52	13.04	-160.81	60.98
	1	6.13	3.65	-190.72	60.51
	5	7.75	5.27	-185.71	60.64
	10	5.40	2.92	-193.80	60.70
II	50	8.88	6.40	-182.75	60.89
	100	8.92	6.44	-183.14	61.04
	500	7.70	5.42	-186.95	61.16
	1000	10.56	8.08	-178.66	61.35
	1	8.58	6.10	-181.77	60.29
	5	10.32	7.85	-176.44	60.45
	10	9.44	6.96	-179.88	60.59
III	50	10.05	7.57	-178.42	60.77
	100	10.75	8.27	-176.68	60.95
	500	9.39	6.92	-181.59	61.06
	1000	7.77	5.29	-187.41	61.17
	1	6.85	4.37	-186.41	59.95
	5	6.03	3.55	-189.85	60.15
	10	5.64	3.16	-191.32	60.19
IV	50	5.64	3.15	-191.35	60.21
	100	5.75	3.27	-191.22	60.28
	500	5.42	2.94	-193.28	60.57
	1000	4.33	1.85	-198.21	60.95
	1	6.73	4.25	-189.62	60.78
	5	5.46	2.98	-194.13	60.86
	10	5.66	3.18	-193.78	60.95
V	50	5.87	3.39	-193.38	61.05
	100	6.44	3.96	-191.84	61.16
	500	8.69	6.21	-185.04	61.38
	1000	7.95	5.47	-187.87	61.48
	1	6.69	4.21	-186.72	59.88
	5	5.87	3.39	-190.14	60.08
	10	5.65	3.17	-191.01	60.13
VI	50	6.95	4.47	-188.79	60.76
	100	5.59	3.12	-191.50	60.21
	500	5.52	3.04	-192.69	60.49
	1000	4.06	1.58	-198.82	60.86

The effect of temperature on the Cu electropolishing rate in absence and presence of amino acids was determined in the temperature range of 25–40 ^{o}C and illustrated in Table 1. It was observed

that the electropolishing rate decrease with temperature for different concentrations of organic additives. Table 2 gives the variation of (%IE) with temperature. The dependence of corrosion rate on temperature can be expressed by the Arrhenius equation [39]:

$$\ln K = -E_a / RT + \ln A \qquad (13)$$

where, K is the reaction rate, A is constant, E_a is the activation energy of the copper dissolution reaction, T is the absolute temperature and R is the universal gas constant. Values of E_a that have been derived from the slopes of Arrhenius plots are given in Table 4.

It is obviously seen that the E_a values in absence and presence of amino acids are less than < 28and kJ. mol^{-1}, also indicating that the diffusion processes are controlling the corrosion reaction [40]. The activation parameters for the corrosion process were calculated from Arrhenius type plot according to the following equations [41, 42]:

$$\Delta H^* = E_a - RT \text{ (kJ. mol}^{-1}\text{)} \qquad (14)$$

$$\Delta G^* = RT (\ln(k_B/h) - \ln (K/T) \text{ (kJ. mol}^{-1}\text{)} \qquad (15)$$

$$\Delta S^* = (\Delta H^* - \Delta G^*) / T \text{ (kJ. mol}^{-1}\text{. K)} \qquad (16)$$

where, k_B is the Boltzman constant ($1.380x10^{-23}$ J/K), h is the Plank's constant ($6.626x\ 10^{-34}$ J.s), R is the universal gas constant (8.314 J/ K. mol), K is the rate constant, ΔG^* is the free energy of activation, ΔH^* is the enthalpy of activation, ΔS^* is the entropy of activation and E_a is the apparent activation energy. The data of the activation parameters for the corrosion process are presented in Table 4.

The negative values of ΔS^* pointed to a greater order produced during the process of activation. This can be achieved by the formation of activated complex represents association or fixation with consequent loss in the degree of freedom of the system during the process. ΔG^* values show limited increase with rise in the concentration of amino acids i.e: ΔG^* values of the inhibited systems were more positive than that for the uninhibited systems revealing weak dependence of ΔG^* on the composition of the amino acids can be attributed largely to the general linear composition between ΔH^* and ΔS^* for the given temperature [43].

3.6. Effect of stirring and applications of dimensional analysis

The effect of speed of rotation on the rate of electropolishing can also be used to determine whether the electropolishing process is a diffusion or chemical controlled process. If the rate of

electropolishing increases by increasing the speed of rotation, then the reaction is diffusion controlled. However, the rate of corrosion is independent on the rotation, so the reaction is likely to be chemically controlled [44].

The angular velocity ω is given by:

$$\omega = (2\pi \text{ rpm}) / 60 \qquad (17)$$

Fig. 7 gives the relation between the limiting current density and the angular velocity, $\omega^{0.7}$ for RCE at 25°C for different concentrations of organic additives used. Straight lines were obtained and the limiting current increases by increasing the rotation which indicates that corrosion reaction of copper is diffusion controlled process. The diffusion coefficient, D(cm^2 s^{-1}), of Cu^{2+} ions in different solutions was determined from the values of limiting current density, as shown in Table 5, using Eisenberg equation [45]:

$$i_L = knFC_b d^{-0.3} \upsilon^{-0.344} D^{0.644} U^x \qquad (18)$$

where k = 0.0791 and x = 0.7 , n is the number of electrons involved in a redox process, F is Faraday's constant (Amp s mol^{-1}), n F is called "Faradaic equivalence", C_b is the bulk concentration (mol cm^{-3}), U is the electrode peripheric velocity = ωr in cm rad s^{-1} (r is the radius in cm), d is the characteristic length of the rotating cylinder, and υ is the kinematic viscosity in stoke (υ = η/ρ) where η is viscosity in poise and ρ is density g cm^{3-} [46].

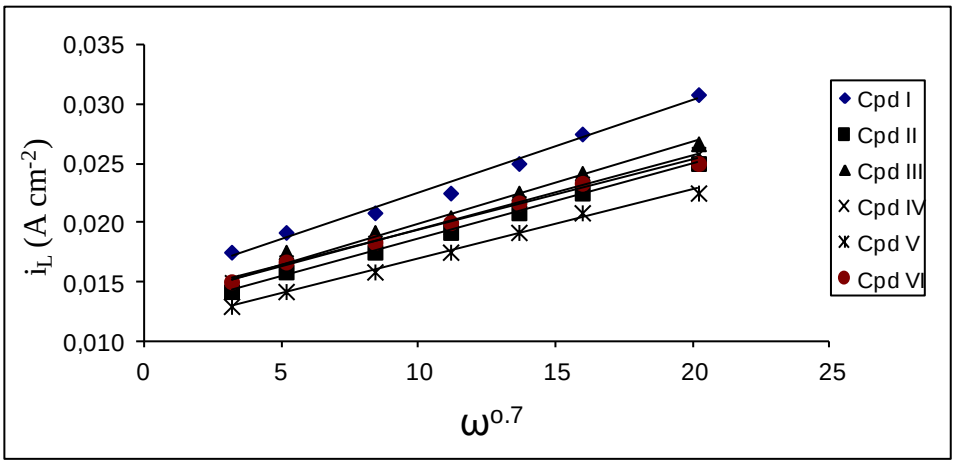

Figure 7. The relation between i_L and $\omega^{0.7}$ for cylinder at 25 °C.

The diffusion coefficient; D, of Cu^{2+} ions in solutions containing amino acids increases due to decrease in interfacial viscosity (η) in accordance [47] with the Stokes-Einstein equation [33]:

$$\eta D / T = \text{Const.} \quad (19)$$

where η is the viscosity of solution (cm poise) , D is the diffusion coefficient of copper ions ($cm^2 s^{-1}$) and T is the absolute temperature (K).

Table 5. Physical properties η, ρ and D used in calculated dimensionless groups for Cu- Cylinder.

Conc.x10^6(mol/l)	i_L(Acm^{-2})	rpm	D(cm^2 s^{-1})	η	ρ	Conc.x10^6(mol/l)	i_L(Acm^{-2})	rpm	D(cm^2 s^{-1})	η	ρ
			I						***II***		
1	1.75E-02	50	1.43E-05	1.65	1.06	1	0.01417	50	6.44E-06	1.10	1.70
5	1.92E-02	100	8.08E-06	1.72	1.02	5	0.01583	100	3.41E-06	1.08	1.85
10	2.08E-02	200	4.59E-06	1.89	1.00	10	0.0175	200	1.78E-06	1.06	2.00
50	2.25E-02	300	3.57E-06	2.10	0.98	50	0.01917	300	1.27E-06	1.04	2.10
100	2.50E-02	400	3.15E-06	2.19	0.97	100	0.02083	400	1.03E-06	1.03	2.20
500	2.75E-02	500	2.88E-06	2.21	0.97	500	0.0225	500	8.83E-07	1.02	2.30
1000	3.08E-02	700	2.54E-06	2.47	0.96	1000	0.025	700	6.94E-07	1.01	2.45
Conc.x10^6(mol/l)	i_L(Acm^{-2})	rpm	D(cm^2 s^{-1})	η	ρ	Conc.x10^6(mol/l)	i_L(Acm^{-2})	rpm	D(cm^2 s^{-1})	η	ρ
			III						***IV***		
1	1.42E-02	50	1.11E-05	1.42	1.10	1	1.50E-02	50	1.05E-05	1.50	1.10
5	1.75E-02	100	6.62E-06	1.63	1.08	5	1.67E-02	100	5.89E-06	1.53	1.09
10	1.92E-02	200	3.94E-06	1.81	1.01	10	1.83E-02	200	3.38E-06	1.59	1.03
50	2.04E-02	300	2.99E-06	2.00	0.98	50	1.96E-02	300	2.66E-06	1.86	1.01
100	2.25E-02	400	2.65E-06	2.15	0.98	100	2.17E-02	400	2.35E-06	1.93	0.98
500	2.42E-02	500	2.38E-06	2.14	0.95	500	2.33E-02	500	2.16E-06	2.05	0.96
1000	2.67E-02	700	2.02E-06	2.42	0.96	1000	2.58E-02	700	1.85E-06	2.20	0.94
Conc.x10^6(mol/l)	i_L(Acm^{-2})	rpm	D(cm^2 s^{-1})	η	ρ	Conc.x10^6(mol/l)	i_L(Acm^{-2})	rpm	D(cm^2 s^{-1})	η	ρ
			V						***VI***		
1	1.29E-02	50	8.22E-06	1.51	1.13	1	1.50E-02	50	1.09E-05	1.62	1.11
5	1.42E-02	100	4.75E-06	1.65	1.10	5	1.67E-02	100	6.32E-06	1.75	1.10
10	1.58E-02	200	2.79E-06	1.78	1.08	10	1.83E-02	200	3.64E-06	1.85	1.05
50	1.75E-02	300	2.25E-06	1.95	1.04	50	2.00E-02	300	2.83E-06	1.97	1.01
100	1.92E-02	400	1.95E-06	2.00	1.01	100	2.17E-02	400	2.46E-06	2.10	0.98
500	2.08E-02	500	1.77E-06	2.05	1.01	500	2.33E-02	500	2.21E-06	2.15	0.97
1000	2.25E-02	700	1.44E-06	2.15	0.98	1000	2.50E-02	700	1.76E-06	2.24	0.95

The mass transport to an inner rotating cylinder electrode in turbulent flow system may be described by empirical dimensionless.

$$Sh = a\, Re^{\,b}\, Sc^{\,c} \quad (20)$$

where Sh, Re and Sc are the Sherwood (Sh = k L/ D), k is mass transfer coefficient, cm s^{-1} ($k = i_L/zFC_{Cu^{2+}}$ where i_L is the limiting current density, $C_{Cu^{2+}}$ is saturation solubility of copper sulphate, z is the valance, F is Faraday's constant in A s mol^{-1}), L is length of cylinder, cm and D is diffusion coefficient, cm^2 s^{-1}, Reynolds (Re = UL/ υ) , υ is kinematic viscosity, cm^2s^{-1} and U is rotation velocity = ωr, cm s^{-1}, (Sc = υ / D) numbers, respectively and a and b are empirical constants, c= 0.33 indicating forced convection regime. As shown in Fig. 8, by plotting log $Sh/(Sc^{0.33})$ against log Re, a straight line was obtained its slope gave the constant "b" while the intercept gives the constant "a".

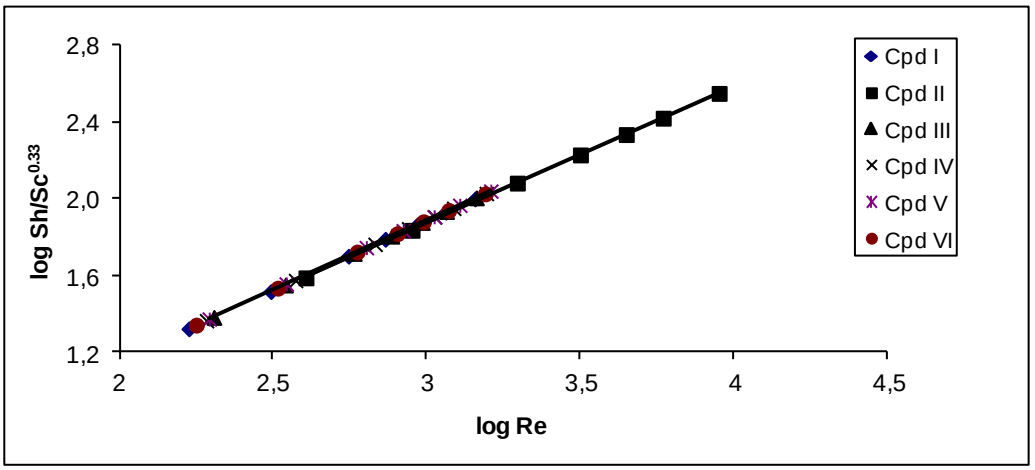

Figure 8. The over all correlation between log $Sh/(Sc)^{0.33}$ and log Re for all amino acids at 25 ^oC.

The over all correlation for all amino acids used as shown in Fig.8 is given by the following equation:

$$Sh = 0.53\ Re^{0.72}\ Sc^{0.33}$$

The exponent of Re in last equations denotes a highly turbulent flow, which agree with the mass transfer study in aqueous media [28, 29, 47].

3.7. Quantum chemical study

The corrosion inhibition efficiencies of the investigated inhibitors were determined experimentally with expected variation in their values. It was found that histidine, cysteine and phenyl alanine compounds have higher inhibition efficiencies than those of proline, alanine and glycine.

Accordingly, quantum chemical calculations were performed to investigate the effect of structural parameters on the inhibition efficiency of inhibitors. Geometric and electronic structures of the inhibitors were calculated by the optimization of their bond lengths, bond angles and dihedral angles. Quantum chemical parameters obtained from the calculations which are responsible for the inhibition efficiency of inhibitors, such as the energies of the highest occupied molecular orbital (E_{HOMO}), energy of the lowest unoccupied molecular orbital (E_{LUMO}), the separation energy (E_{LUMO}-E_{HOMO}), ΔE, representing the function of reactivity, the dipole moment (μ), total energy (E_t), hardness (η), softness (σ), summation of the total negative charges on atoms over the skeleton of the molecule (TNC), and molecular volume of molecule (M.V), are collected in Table 6.

The use of Mulliken population analysis to estimate the adsorption centers of inhibitors has been widely reported and it is mostly used for the calculation of the charge distribution over the whole skeleton of the molecule [48-53]. There is a general consensus by several authors that the more negatively charged heteroatom is the more, it can be adsorbed on the metal surface through donor–acceptor type reaction. The calculated Mulliken charges showed that there is more than one active center. Variation in the inhibition efficiency of the inhibitors depends on the presence of electronegative O, S and N atoms as substituents in their molecular structure. The sites of ionic reactivity could be estimated from the net charges on a molecule. Thus, the calculations showed that the inhibitors with higher inhibition efficiency such as histidine has five adsorption centres with high negative charge density (two oxygen and three nitrogen atoms), while the cysteine (two oxygen, nitrogen and sulfur atoms) and phenylalanine (two oxygen, nitrogen atoms and aromatic phenyl ring) inhibitors have four ones, Fig.9 [a, b, c]. Meanwhile, the inhibitors with lower inhibition such as proline, alanine and glycine have three adsorption centres (two oxygen and nitrogen atoms), Fig.9 [d, e, f], which agrees with the experimental observations. The above conclusion was confirmed by calculating TNC, where the more active sites have the molecule, the higher is TNC and the higher is the inhibition efficiency. The calculations showed that the inhibitors with the highest inhibition efficiency have the highest TNC values which agree well with the experimental observations, Table 6.

According to the frontier molecular orbital theory, FMO, the chemical reactivity is a function of interaction between HOMO and LUMO levels of the reacting species [54]. The E_{HOMO} indicates the ability of the molecule to donate electrons to an appropriated acceptor with empty molecular orbitals and E_{LUMO} indicates its ability to accept electrons. The lower is the value of E_{LUMO}; the more is the ability of the molecule to accept electrons [55]. The higher is the value of E_{HOMO} of the inhibitor, the greater is its ease of offering electrons to the unoccupied d-orbital of metal surface and the greater is its inhibition efficiency. The calculations showed that the lowest energy E_{HOMO} is assigned for the glycine compound which is expected to have the lowest corrosion inhibition among the investigated compounds. On the other hand, the phenyl alanine destabilized the HOMO level by 0.752 eV to increase its donation to the metal surface and increases its tendency to adsorb on the metal surface and accordingly has high inhibition efficiency. This expectation is in a good agreement with the experimental observations.

It was found that the variation of the calculated LUMO energies among all investigated inhibitors is rulelessly, and the inhibition efficiency is misrelated with the changes of the E_{LUMO}, Table 6. The HOMO–LUMO energy gap, ΔE approach, which is an important stability index, is applied to develop theoretical models for explaining the structure and conformation barriers in many molecular systems. The smaller is the value of ΔE, the more probable that the compound has inhibition efficiency [56-58]. It was shown from Table 6 that glycine molecule has the highest HOMO–LUMO gap, 10.388 eV, eV compared with the other molecules. Meanwhile, the inhibitors with high inhibition efficiency have low energy gaps, Table 6. Accordingly, it could be expected that glycine inhibitor has less inclination to adsorb on the metal surface than the other molecules. Also, it was shown from the calculations that the molecules with the high inhibition of corrosion have lower total energy E_t than those with low inhibition efficiency, Table 6, which agrees well with the experimental observations.

The dipole moment, μ, the first derivative of the energy with respect to an applied electric field, was used to discuss and rationalize the structure [59]. There is a lack of agreement in the literature on the correlation between μ and inhibition efficiency [60, 61]. The theoretical results indicate that no significant relationship was detected between μ and inhibition efficiency. However, the lowest value of μ was shown for glycine which has the lowest inhibition efficiency.

Absolute hardness, η and softness, σ are important properties which measure both the stability and reactivity of a molecule. A hard molecule has a large energy gap and a soft molecule has a small energy gap. Soft molecules are more reactive than hard ones because they could easily offer electrons to an acceptor.

For the simplest transfer of electrons, adsorption could occur at the part of the molecule where σ, which is a local property, has the highest value [62]. In a corrosion system, the inhibitor acts as a Lewis base while the metal acts as a Lewis acid, respectively. Bulk metals are soft acids and thus soft base inhibitors are most effective for acidic corrosion of those metals. Accordingly, it is concluded that glycine inhibitor with the lowest σ value has the lowest ability inhibition efficiency, Table 6, which is in a good agreement with the experimental data.

Table 6. The calculated quantum chemical parameters for the investigated inhibitors.

Molecule	E_{HOMO} (eV)	E_{LUMO} (eV)	ΔE (eV)	μ (D)	E_t (eV)	M.V. A^3	TNC (e)	η (eV)	σ (eV^{-1})
Histidine	-9.511	0.405	9.916	3.082	-1978.869	180.000	-2.675	4.958	0.202
Cysteine	-9.615	-0.236	9.379	4.191	-1400.142	139.090	-2.187	4.690	0.213
Phenyalanine	-9.415	0.189	9.604	1.411	-2014.439	205.750	-2.671	4.802	0.208
Proline	-9.373	0.383	9.756	1.821	-1498.032	141.810	-2.180	4.878	0.205
Alanine	-10.028	0.302	10.330	1.122	-1225.961	113.270	-2.030	5.165	0.194
Glycine	-10.167	0.221	10.388	1.050	-1076.070	90.120	-1.752	5.194	0.192

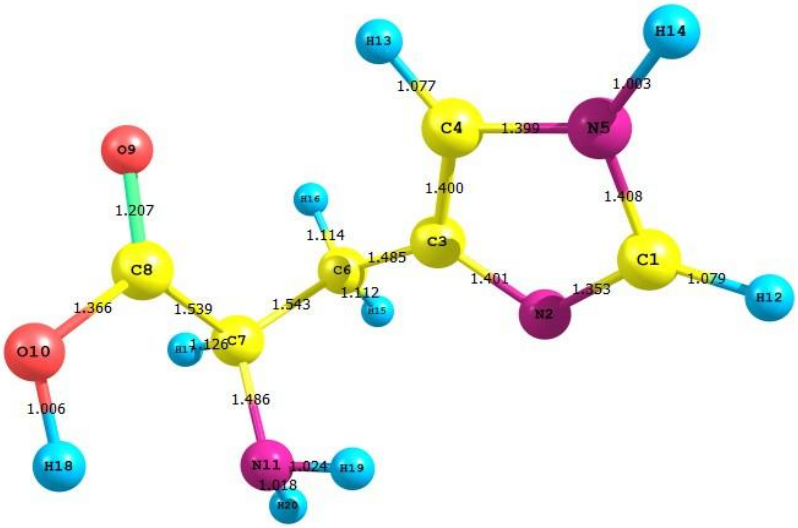
H13
1.077
H14
1.003
C4
1.399
N5
1.400
1.408
O9
1.207
H16
1.114
C3
1.485
C1
1.079
H12
C8
C6
1.112
1.401
1.353
N2
1.366
1.539
1.543
H15
O10
H17
1.126
C7
1.486
1.006
H18
N11
1.024
H19
1.018
H20

A

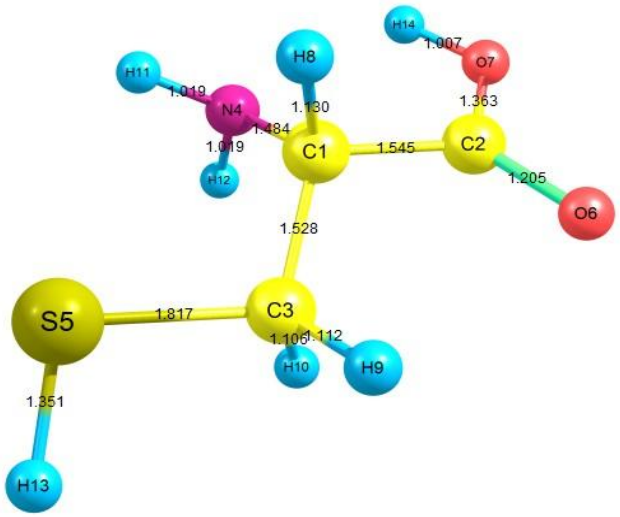
H14
1.007
O7
H8
H11
1.019
1.130
1.363
N4
1.484
1.019
C1
1.545
C2
H12
1.205
O6
1.528
S5
1.817
C3
1.106
1.112
H10
H9
1.351
H13

B

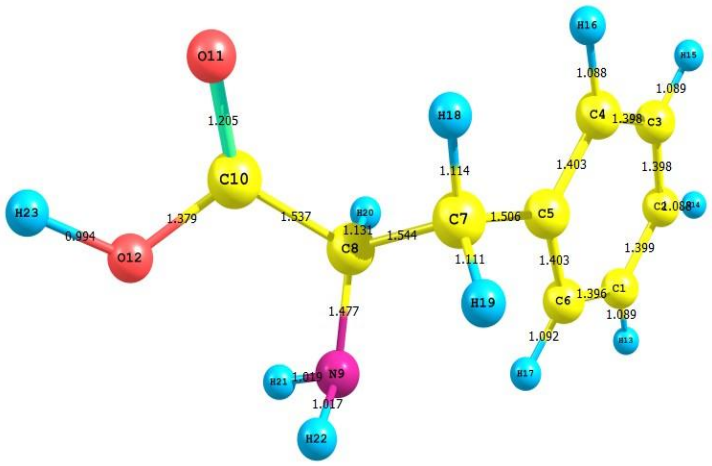
O11
H16
1.088
H15
1.089
1.205
C4
1.398
C3
H18
1.403
1.398
1.114
C10
H23
1.379
1.537
H20
1.131
C7
1.506
C5
C2
1.088
H14
0.994
O12
1.544
C8
1.111
1.403
1.399
H19
C6
1.396
C1
1.089
1.477
1.092
H13
H17
H21
1.018
N9
1.017
H22

C

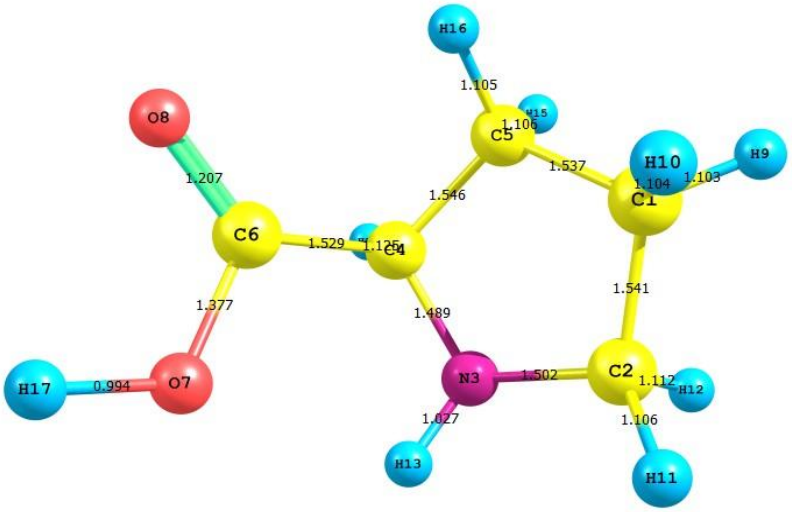

D

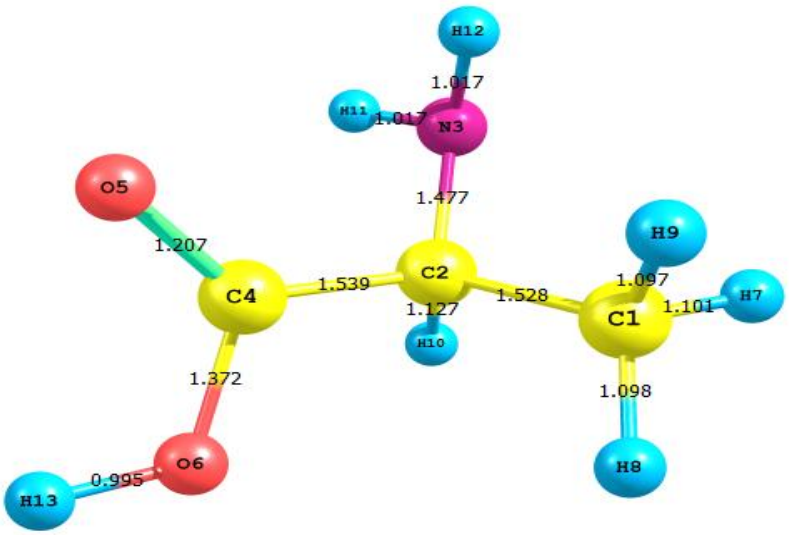

E

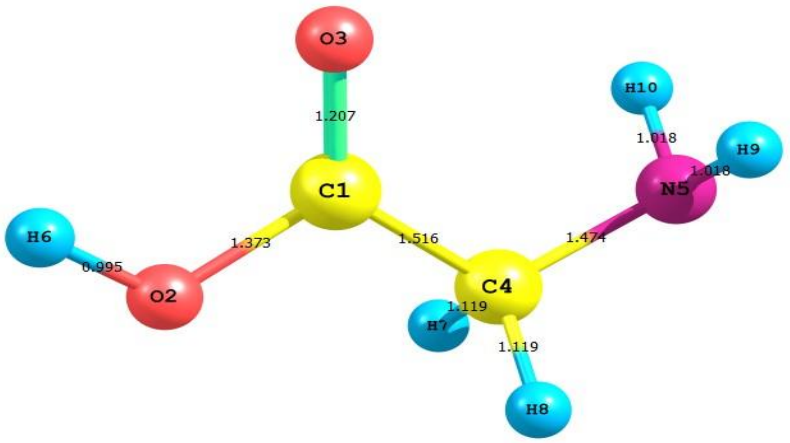

F

Figure 1. The calculated optimized molecular structures of (a) histidine, (b) cysteine, (c) phenyl alanine, (d) proline, (e) alanine and (f) glycine.

The inhibition efficiency increases as the volume of the molecules increases due to the increase of the contact area between molecule and surface. It was shown from the calculations that glycine has the lowest molecular volume with a value equals 90.120 A^3, which is proportional to the polarisability leading to decreasing its adsorption on the metal surface and decreasing its inhibition efficiency.

4. CONCLUSIONS

- Corrosion of copper surface is influenced by type of cell divided or undivided cell, electrode height, temperature, type and concentrations of amino acids and rpm of rotating copper cylinder.
- Amino acids acts as strong inhibitor for copper corrosion in phosphoric acid and its adsorption obey Temkin and Kinetic adsorption isotherm.
- By increasing speed of rotation, the reaction rate increase, this indicates that the reaction is diffusion control.
- For RCE, the exponent of Re in mass transfer correlation denotes a highly turbulent flow.
- Quantum chemical calculations showed an agreement between quantum chemical parameters related to the electronic structure of the investigated compounds and their ability to inhibit the corrosion process. The experimental inhibition efficiencies are closely related to the quantum chemical parameters such as E_{HOMO}, ΔE, E_t, σ, η, TNC, MV. No significant relationship was found between E_{LUMO} and μ with the experimental inhibition efficiency.

Finally, this study displays a good correlation between the theoretical and experimental data which confirms the reliability of the quantum chemical methods to study the inhibition of corrosion of metal surfaces.

References

1. A.M. Awad, N.A. Abdel Ghany and T.M. Dahy, *J. Appl. Surf. Sci*., 256 (2010) 4370.
2. S. Abd El-Wanees and E.E. Abd El-Aal, *Corros. Sci.*, 52 (2010) 338.
3. X. Li, S. Deng, G. Mu, H. Fu and F. Yang, *Corros. Sci.*, 50 (2008) 420.
4. V.R. Saliyan and V. Adhikari, *Corros. Sci.*, 50 (2008) 55.
5. A.Popova, M. Christov, S. Raicheva and E. Sokolova, *Corros. Sci.*, 46 (2004) 1333.
6. L. Tang, X. Li, L. Li and G. Liu, *Surf. Coat. Technol*., 201 (2006) 384.
7. E.E. Abd El-Aal, W. Zakria, A. Diab and S.M. Abd El-Haleem, *Anti-Corros.*, 48 (2001) 181.
8. E.E. Abd El-Aal, W. Zakria, A. Diab and S.M. Abd El-Haleem, *J. Mater. Eng. Perform.*, 12 (2003) 172.
9. T.T. Qin, J. Li, H.Q. Luo, M. Li and N.B. Li, *Corros. Sci.*, 53 (2011) 1072.
10. Y.S. Li, W.J. Lu, Y. Wang and T. Trana, *Spectrochim. Acta A*, 73 (2009) 922.
11. Z.X. Kang, Q. Ye, J. Sang and Y.Y. Li, *J. Mater. Process. Technol.*, 209 (2009) 4543.
12. A.Popova, *Corros. Sci.*, 49 (2007) 2144.
13. M.N.H. Moussa, A.A. El-Far and A.A. El-Shafi, *Mater. Chem. Phys.*, 105 (2007) 105.
14. X. Li, S. Deng, H. Fu and G. Mu, *Corros. Sci.*, 51 (2009) 2639.

15. G.M. El-Subruiti and A.M. Ahmed, *Portug. Electrochim. Acta*, 20 (2002) 151.
16. M.K. Awad, R.M. Issa and F.M. Atlam, *Mater. Corros*., 60 (2009) 813.
17. M.K. Awad, *J. Electroanal. Chem*., 567 (2004) 219.
18. R.M. Issa, M.K. Awad and F.M. Atlam, *Appl. Surf. Sci.*, 255 (2008) 2433.
19. M.K. Awad, F.M. Mahgoub and M.M. El-iskandrani, *J. Mol. Struct. (THEOCHEM)*, 531 (2000)105.
20. M.S. Masoud, M.K. Awad, M.A. Shaker and M.T. El-Tahawy, *Corros. Sci*., 52 (2010) 2387.
21. R.M. Issa, M.K. Awad and F.M. Atlam, *Mater. Corros.*,10 (2009) 60.
22. M.K. Awad, M.R. Mustafa and M.M. Abo Elnga, *J. Mol. Struct. (THEOCHEM)*, 959 (2010) 66.
23. C.R. Wilke, M. Eisenberg and C.W. Tobias, *J. Electrochem. Soc.*, 102 (1953) 531.
24. R.G. Parr and R.G. Pearson, *J. Am. Chem. Soc.*, 105 (1983) 7512.
25. R.G. Pearson, *Inorg. Chem*., 27 (1988) 734.
26. G.M. El-Subruiti, A.M. Ahmed and M.G. Koretam, *Bull. Electrochem.*, 19 (2003) 185.
27. S.T. Mayer, R.J. Contolini and A.F. Bernhardt, *J.Electrochem. Soc.*, 141 (1994)2503.
28. H.H. Abdel-Rahman, *J. Disper. Sci. Technol.*, 31 (2010) 1740.
29. N.M. Elmalah, A.M. Ahmed and L.F. Gado, *J. Disper. Sci. Technol.*, 31 (2010) 1579.
30. B. Mansfeld and J.V. Kenle, *Corros. Sci.*, 15 (1975) 767.
31. D. Landolt, *Electrochim. Acta*, 32 (1987) 1.
32. A.A. Taha, S.H. Sallam and A.M. Ahmed, *Anti-Corros. Methods Mater.*, 41 (1994) 10.
A. Einstein, *The Royal society of London* 106 (1924) 724.
33. A.El Warraky, H.A. ElShayeb and E.M. Sherif, *Anti-Corros. Methods Mater.*, 51 (2004) 52.
34. S.A. Umoren, O. Ogbobe, I.O. Igwe and E.F. Ebenso, *Corros. Sci.*, 50 (2008) 1998.
35. A.S. Fouda, M. Abdallah and A. Attia, *Chem. Eng. Comm.*, 197 (2010) 1091.
36. R. Solmaz, G. Kardaş, B. Yazici and M. Erbil, *Colloid Surf. A*, 312 (2008) 7.
37. H.H. Abdel-Rahman, A.M. Ahmed, A.A. Harfoush and A.H.E. Moustafa, *Hydrometallurgy*, 104 (2010) 169.
38. E.A. Noor, *Mater., Mater.Chem.Phys.*, 114 (2009) 533.
39. H. Ashassi-Sorkhabi, B. Shaabani and D. Seifzdeh, *Electrochim. Acta*, 50 (2005) 3446.
40. A.M. Al-Sabagh, N.S. Tantawy, N.M. Nasser and M.R. Mishrif, *J. Disper. Sci. Technol.*, 30 (2009) 1411.
41. G. Moretti., G.T. Quartarone and A. Zingales, *Electrochem. Acta*, 41 (1996) 1971.
42. H.M.A. Soliman, *Appl. Surf. Sci.*, 195 (2002) 155.
43. A.M. Ahmed, A.A.-H. Abdel-Rahman and A.F. El Adl, *J. Disper. Sci. Technol.*, 32 (2011) 453.
44. M. Eisenberg, C.W. Tobias and C. R. Wilke, *J. Electrochem. Soc*., 102 (1955) 415.
45. J.M. Maciel and M.L. Gostinho, *J. Appl. Electrochem.*, 29 (1999) 741.
46. D.R. Gabe and F.C. Wilcox, *J. App. Electrochem.*, 28(1998) 759.
47. F.H. Assaf, M. Abou-Krish, A.S. El-Shahawy, M. Makhlouf and H. Soudy, *Int. J. Electrochem. Sci*,. 2 (2007) 158.
48. R. Hasanov, M. Sadikoglu and S. Bilgic, *Appl. Surf. Sci.*, 253 (2007) 3913.
49. N.K. Allam, *Appl. Surf. Sci.*, 253 (2007) 4570.
50. M. Ozcan, I. Dehri and M. Erbil, *Appl. Surf. Sci.*, 236 (2004) 155.
51. J.M. Roque, T. Pandiyan, J. Cruz and E. Garcl´a-Ochoa, *Corros. Sci.*, 50 (2008) 614.
52. F. Kandemirli and S. Sagdinc, *Corros. Sci.*, 49 (2007) 2118.
53. K. Fukui, *Theory of Orientation and Stereoselection*, Springer-Verlag, New York, 1975.
54. G. Gece, *Corros. Sci.*, 50 (2008) 2981.
55. D.Q. Zhang, L.W. Gao and G.D. Zhou, *Corros. Sci.*, 46 (2004) 3031.
56. G. Gao and C. Liang, *Electrochim. Acta*, 52 (2007) 4554.

57. Y. Feng, S. Chen, Q. Guo, Y. Zhang and G. Liu, *J. Electroanal. Chem.*, 602 (2007)115.
58. N. Khalil, *Electrochim. Acta*, 48 (2003) 2635.
59. L.M. Rodrigez-Valdez, A. Martinez-Villafane, D. Glossman-Mitnik, *J. Mol. Struct. (THEOCHEM,)* 713 (2005) 65.
60. A.Stoyanova, G. Petkova and S.D. Peyerimhoff, *Chem. Phys.*, 279 (2002) 1.
61. S. Martınez, *Mater. Chem. Phys.*, 77 (2002) 97.